Investigation of AC Loss in an impregnated 3-Parallel Strands HTS Coil for a Superconducting Armature of Electrical Machine for Aeronautics

Arthur Jamois-Le Gouguec, Bruno Douine, Paul Gning, Jean Lévêque, Christophe Viguier

Investigation of AC Loss in an impregnated 3-Parallel Strands HTS Coil for a Superconducting Armature of Electrical Machine for Aeronautics

Arthur Jamois–Le Gouguec, Bruno Douine, Paul Gning, Jean Lévêque, Christophe Viguier

***Abstract*—The design of a superconducting armature is currently one of the major challenges for the development of a cryogenic turboelectric chain for aeronautics. To limit the voltage rise in aircraft, HTS coils are designed with parallel strands and must withstand both thermal constraints related to the presence of AC losses and mechanical constraints during operation. In this study, the AC losses of an impregnated 3-parallel strands racetrack double pancake HTS coil were investigated for currents and frequencies ranging from 30 to 150 A and from 40 to 440 Hz, respectively. Experimental results show that despite an overall hysteresis loss behavior, mechanical losses of vibrational origin seem to be part of the loss balance, particularly at low current and high frequency where they appear to be preponderant.**

***Index Terms*—Superconducting electrical machine, superconducting armature, vibrations, AC losses, REBCO tape, electric aircraft.**

I. Introduction

The aeronautics sector currently contributes from 2 to 4 % of total anthropogenic greenhouse gas emissions. Despite the Covid-19 crisis, air traffic returned to its original level in 2024 and, with an expected 2 % annual growth, the number of passengers is expected to double by 2045 [1]. To meet the zero emissions objectives set for 2050, the electrification of aircraft is a major opportunity to decarbonize the industry [2]. Among the potential low-carbon fuels, liquid hydrogen (LH_2) at 20 K enables the design of a new cryogenic propulsion system that benefits from the onboard cold source, but requires significant structural changes [3]. Although such a technological breakthrough would bring performance gains, it requires high-power, high-efficiency electrical components to avoid significantly degrade the overall propulsion chain yield [4]. High-temperature superconductors (HTS) of REBCO type, with a critical temperature exceeding 90 K and current densities up to 1000 A/mm^2, appear as attractive candidates for the design of fully superconducting electrical machines with high efficiency and high specific power. The HTS rotor having been studied in the past, several projects are now focusing on the design of an HTS armature made complex by the presence of AC losses induced by the AC transport current and the rotating magnetic field [5]–[7]. Conventionally, the winding is also impregnated to withstand mechanical stresses that can cause additional losses [8]. Several studies have investigated the AC losses of impregnated HTS coils up to currents and frequencies reaching 150 A and 1 kHz [9]–[13].

This study takes place within a project to design a superconducting armature for an electrical machine for an aeronautical application, in line with the work already performed on a superconducting rotor [14], [15]. The design and the characterization of an impregnated HTS racetrack double pancake coil made from second-generation REBCO HTS coated conductors is presented. Three strands were arranged in parallel to increase the current capacity and limit the voltage rise, the use of high voltage in an aerospace environment being able to lead to tracking, partial discharge or breakdown [16]. Sections II and III successively present the design and specifications of the coil and the experimental procedures for characterization in critical current and AC losses, and the results are analyzed in Section IV.

II. Coil description

The experimental coil is designed with a 4 mm-wide second-generation insulated superconducting REBCO tape from Fujikura Ltd. (product reference FESC-SCH04). The total thickness is 110 μm and the critical current at 77.3 K in self-field has been measured beforehand at 244 A on a 10 cm sample. The tape and coil specifications are listed in the Table I and Table II, respectively.

Table I
Fujikura FESC-SCH04 tape characteristics.

Parameter	Description	Value
w [mm]	Width	4
h [mm]	Thickness	0.11
I_c [A]	Critical current @ 77 K	244
n [-]	Power law index	29.0

Three parallel tapes were co-wound into a racetrack coil according to the double pancake winding method. No transposition is performed during the winding and the coil is impregnated with a epoxy-hardener mixture. Each strand measures 5.1 $\pm$ 0.1 m in total length and is numbered for the study according to Fig. 1. The number of turns is 12, and the straight segment length of the coil is 130 mm for a internal coil head radius of 25 mm.

Arthur Jamois–Le Gouguec, Paul Gning and Christophe Viguier are with the Electrical and Electronic Systems Research Department, SAFRAN TECH, 1 rue des Jeunes bois - Châteaufort Magny-les-Hammeaux, 78772, France (e-mail: arthur.jamois@safrangroup.com; paul.gning@safrangroup.com; christophe.viguier2@safrangroup.com)

Arthur Jamois, Bruno Douine and Jean Lévêque are with the Research Group in Electrical Engineering and Electronics of Nancy (GREEN), University of Nancy, F-54506 Vandoeuvre-lès-Nancy, France (e-mail: bruno.douine@univ-lorraine.fr; jean.leveque@univ-lorraine.fr).

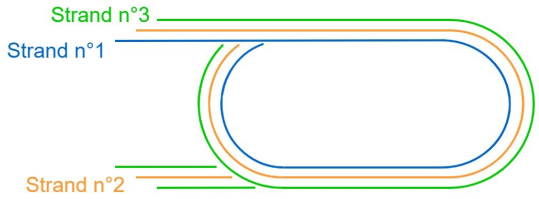

Figure 1. Sketch of the coil and strands numbering.

The coil inductance measurement has been performed as the same time as the AC loss measurement. First and foremost, only one strand is supplied to measure its self inductance and the mutual inductances. Secondly, the strands are supplied identically and separately (the experimental procedure is depicted in Section III). The measurements result in equal self- and mutual inductances equal to each other and between strands (i.e. $L = M$), and the coil inductance is 30.2 µH.

Table II
COIL CHARACTERISTICS.

Parameter	Characteristic/Value
Coil configuration	Racetrack coil
Winding method	Double-pancake winding
Number of parallel conductors	3
Number of turns	12 (= 6 + 6)
Strand's length (between voltage tapes)	5.1 ± 0.1 m
Coil inductance	30.2 µH

Fig. 2 shows the experimental setup of the racetrack double pancake coil (RDPC). The coil is fixed on a fiberglass support. Each strand is supplied independently through respective copper connections to ensure an equal current distribution. Voltage measurements are carried out with copper clamps on the bared tape surface.

III. EXPERIMENTAL PROCEDURES

The critical current of each strand is determined according to the normalized voltage criterion of 1 $\mu V/cm$. The experimental coil is immersed in liquid nitrogen (LN_2), and the strands are powered independently with a PSB 10080-1000 4U 3000W from Elektro-Automatik, a TDK-LAMBDA GEN3300W, and a Xantrec XFR 7.5-300 controlled by a Power Supply Programmer Model 420 from American Magnetics Inc. The voltage measurements is realized with Keithley nanovoltmeters 2182 and 2182A, where the average value and its standard deviation is obtained from a sampling of 600 measurements fixed at a medium rate.

The AC loss measurements are performed using the lock-in amplifier method [17]. The electrical schematic of the experimental setup is shown in Fig. 3. A 55 kW Pacific SmartRegen 3550 AZX bidirectional AC/DC generator, set in single-phase mode, powers each strand simultaneously and independently. No phase shift is therefore introduced between the three phases. The coil voltages are measured with RS-SI 7005 differential probes connected to a MFLI 500 kHz - 5 MHz from Zurich Instruments. The current and frequency references are obtained with a Hioki 3275 Clamp On Probe

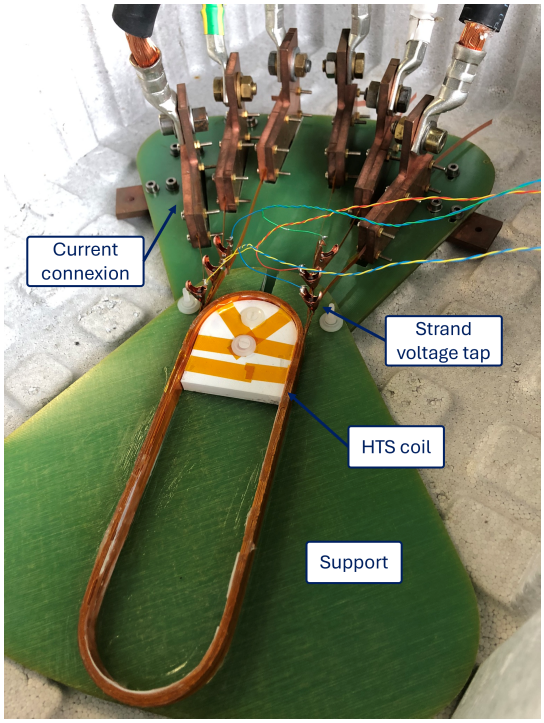

Figure 2. Racetrack double pancake coil connections for AC loss measurement.

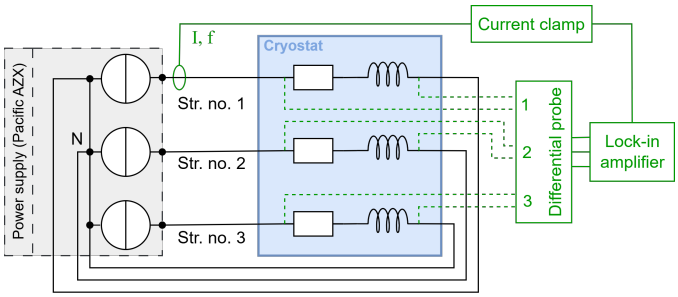

Figure 3. Schematic of the experimental setup of AC loss measurement.

connected on the cable power of one of the phase, considered to be identical. The Fig. 4 shows the power supply side setup where the experiment is controlled from the computer using the dedicated interfaces of each device.

IV. RESULTS AND DISCUSSION

A. Critical current characterization

Fig. 5 shows strand voltages in function of the DC current. The red dotted line indicates the voltage at which the critical strand current is reached. A first observation can be made regarding characteristics of the critical current: strands no. 1 and no. 2 exhibit similar behavior while strand no. 3 presents an identifiable resistive influence visible through an earlier voltage rise and a less pronounced slope. Table III records the critical current I_c and the power law index n, which will be noted I_{c_i} and n_i for the corresponding strand no. i. n_3 corresponds thereby to half of n_1 and n_2, concluding that a defect either in the structure of the tape or introduced during the winding process is at the origin of this resistive behavior.

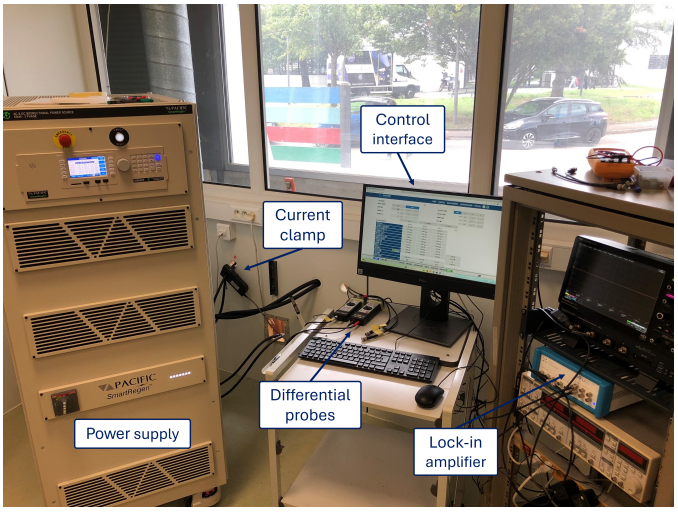

Figure 4. Power supply side setup of AC loss measurement.

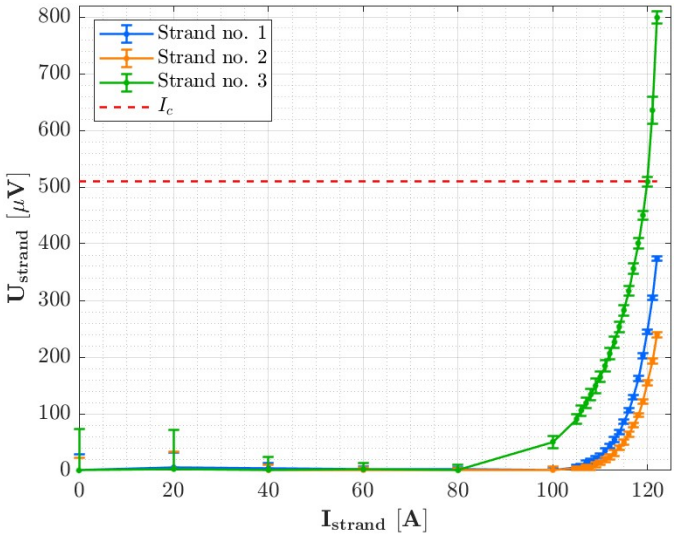

Figure 5. Strands critical current characterization.

It can be added that n_1 and n_2 are less than of the power law index of a single tape shown in Table I due to a larger magnetic field of the coil. Despite this difference between strands, the critical currents are relatively close, within a range of 5 A. Since the experiment has been stopped before reaching I_{c_1} and I_{c_2} in order to avoid a quench in the strand no. 3, the latter have been identified thanks to a power law on the corresponding part of the characteristic. Compared to a single tape, strands exhibit an average reduction of 49.7 % on the critical current, mainly due to the magnetic field of the coil.

Table III
COIL STRAND PARAMETERS.

Parameter	Description	No. 1	No. 2	No. 3
I_c [A]	Critical current @ 77.3 K	123	125	120
n [-]	Power law index	25.6	27.6	14.0

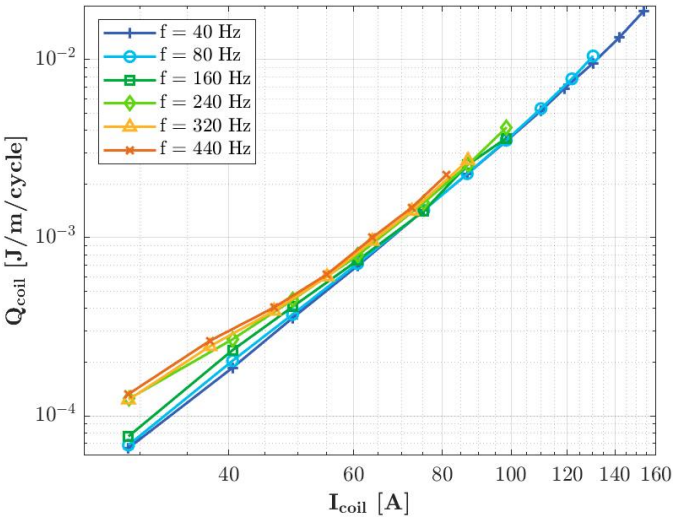

Figure 6. Total energy dissipation of the coil per unit length over a cycle as a function of the total RMS current.

B. AC loss measurement

The AC losses Q_{strand} (J/m/cycle) of each strand are obtained by the following relation:

$$Q_{strand} = \frac{V_{rms} I_{rms}}{Lf} \tag{1}$$

where V_{rms} and I_{rms} stand for the RMS value of the measured voltage and the corresponding current, L the length of the strand and f the operating frequency. Then, they are summed to obtain the total coil losses. The authors observed that the strands exhibit identical losses, with any very small perceptible difference being due to the calibration of the differential probes. Since they are co-wound and have equal inductances, Q_{strand} corresponds to the sum of the losses of each strand. The total energy dissipation of the coil Q_{coil} can therefore be expressed as:

$$Q_{coil} = \sum_{i=1}^{3} Q_i = 3 \times Q_1 \tag{2}$$

where Q_i corresponds to the energy dissipation of the strand no. i. In the case of perfectly balanced transport current between the strands, the energy dissipation of a parallel-stranded HTS RDPC is to some extent a measure of the performances of the least efficient. In a practical approach, Q_{coil} could be obtain from the AC losses of one of the strands multiplied by the number of HTS tape in parallel.

Fig. 6 shows the total energy dissipation per unit length over a cycle of the coil as a function of the total RMS current for frequencies varying from 40 to 440 Hz. The results agree well with each other at middle and high current amplitude, despite a slight upward shift. No frequency dependence is observed, the hysteresis loss is therefore the dominant component of the AC losses for $I_{coil} \geq 60$ A. However, this observation is not valid at low current amplitude, where the characteristics do not exhibit the same behavior depending on the frequency. Two trends can be identified (despite a decrease in measurement

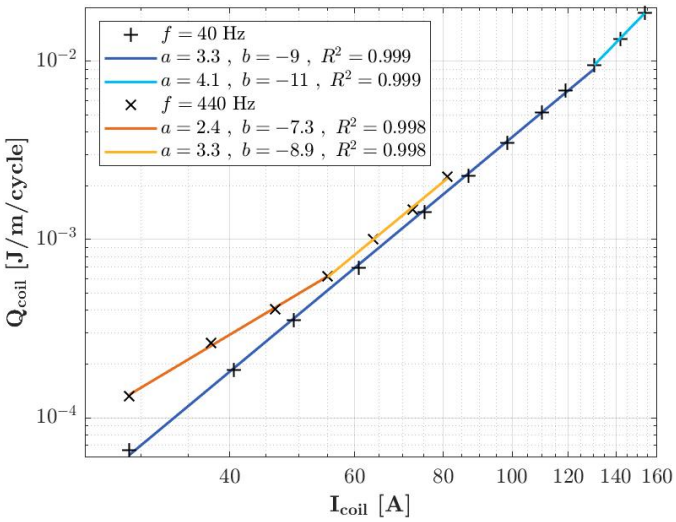

Figure 7. Trend of the energy dissipation of the coil as a function of coil RMS current. The linear regressions of type $y = 10^b \times x^a$ highlight a change in the AC loss behavior regarding the current I_{coil} and the frequency f.

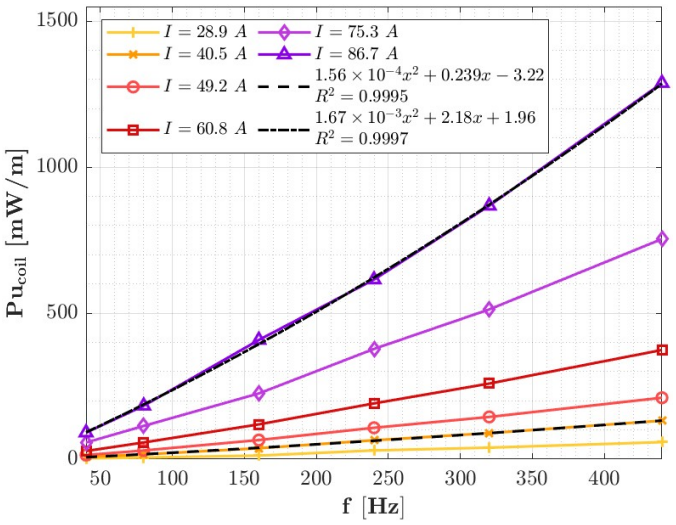

Figure 8. Total power dissipation of the coil per unit length as a function of the frequency. Two trend lines for $I = 40.5$ A and $I = 86.7$ A were plot in order to highlight the f^2 dependency of the AC loss behavior.

accuracy at low current), with a clear change happening between 160 Hz et and 240 Hz.

To characterize these inflection changes, linear regressions (LR) corresponding to a power law of type $y = 10^b \times x^a$ were performed on the curves for different current intervals. Fig. 7 depicts the LR for $f = 40$ Hz and $f = 440$ Hz, since they are representative of the results obtained for $f = \{40, 160\}$ Hz and $f = \{240, 320\}$ Hz, respectively. LR agree well regardless of frequency on an average power lax index a of 3.3 at middle current amplitude, i.e. $I \in [50, 120]$ A. The typical value of the slope corresponding to hysteresis loss in the superconducting layer is between 3 and 4 (other losses being negligible) [18]. The results obtained are also consistent with the experimental works available in the literature [9], [13]. For 40 and 80 Hz, the slope increases to 4.1 on the last measurement data, which can be interpreted as a decrease in $J_c(B)$, the coil self-field increasing with current. However, it is not possible to conclude on a behavior solely due to hysteresis losses. For current amplitudes below 50 A, the Q_{coil} characteristics for frequencies equal to or greater than 240 Hz exhibit an average slope of 2.4. This change can be attributed to vibration-related phenomena in the coil, since the mechanical vibration are $\propto I^2$ [19].

Fig. 8 shows the power dissipation per unit length of the coil as a function of the frequency. Although below $I = 60$ A the characteristics appear to be linear, trend line estimations resulted in better agreement with a second-order polynomial regression. The trend line equations and correlation coefficients are given in Fig. 8 for the curves $I = 45.5$ A and $I = 86.7$ A. According to the measurements performed by Z.Jiang *et al* on pancake coils made of 2G HTS tapes, no eddy current loss has been observed up to frequencies of approximately 1 kHz [11]. The f^2 dependency hightlighted can therefore be associated to mechanical vibration [8]. This behavior may explain why mechanical losses become significant at low currents, as they increase to squarely with increasing frequency. They are then gradually dominated by hysteresis losses, since these are an order of magnitude less dependent on the transport current ($\propto I^2$ vs $\propto I^3$). The AC loss mechanism for parallel-stranded HTS RDPC could be interpreted as:

$$P_{AC} = P_{HTS} + P_{mech} \tag{3}$$

where P_{HTS} and P_{mech} stand for the hysteresis loss component and the mechanical loss component caused by inter-strand friction, friction with structural materials and/or deformation of the RDPC, respectively.

V. Conclusion

For HTS armature windings of fully superconducting machines for an aeronautical application, we investigated the AC loss mechanism for a 3-parallel strand racetrack double pancake HTS coil. Mechanical vibration were observed during experimental tests despite prior impregnation. The AC losses are dominating by the hysteresis loss in the superconducting layer at middle and high current amplitude, but mechanical losses due to vibration seem to become predominant at low current with increasing frequency. This observation is highlighted by a second-order polynomial trend in loss frequency, suggesting the presence of vibration despite prior impregnation. It is therefore crucial to ensure good mechanical strength - through impregnation and/or mechanical supports - for high-frequency applications of HTS coils to limit the AC losses and to ensure coil stability.

References

[1] B. Graver and J. Mukhopadhaya, "ALIGNING AVIATION WITH THE PARIS AGREEMENT."

[2] J. Amilhat, "Fly the green deal, europe's vision for sustainable aviation, report of the advisory council for aviation research and innovation in europe (ACARE)."

[3] M. Boll, M. Corduan, S. Biser, M. Filipenko, Q. H. Pham, S. Schlachter, P. Rostek, and M. Noe, "A holistic system approach for short range passenger aircraft with cryogenic propulsion system," vol. 33, no. 4, p. 044014, number: 4 Publisher: IOP Publishing. [Online]. Available: https://dx.doi.org/10.1088/1361-6668/ab7779

[4] R. H. Jansen, "Partially turboelectric aircraft drive key performance parameters."

[5] C. C. T. Chow, M. D. Ainslie, and K. T. Chau, "High temperature superconducting rotating electrical machines: An overview," vol. 9, pp. 1124–1156. [Online]. Available: https://www.sciencedirect.com/science/article/pii/S2352484722025628

[6] D. Malkin, "Cryogenic hyperconducting networks and the move to superconducting," EFATS 2022.

[7] E. Nilsson, "Superconductivity & cryogenics for future electric aircraft propulsion," connectus Summer School.

[8] J. F. Gieras, C. Wang, and J. C. Lai, "Noise of polyphase electric motors," p. 333, ISBN: 9781420027730. [Online]. Available: https://www.academia.edu/83072864/Noise_of_Polyphase_Electric_Motors

[9] F. Grilli and S. P. Ashworth, "Measuring transport AC losses in YBCO-coated conductor coils," vol. 20, no. 8, p. 794. [Online]. Available: https://doi.org/10.1088/0953-2048/20/8/013

[10] J. Šouc, E. Pardo, M. Vojenčiak, and F. Gömöry, "Theoretical and experimental study of AC loss in high temperature superconductor single pancake coils," vol. 22, no. 1, p. 015006. [Online]. Available: https://doi.org/10.1088/0953-2048/22/1/015006

[11] Z. Jiang, N. J. Long, R. A. Badcock, M. Staines, R. A. Slade, A. D. Caplin, and N. Amemiya, "AC loss measurements in pancake coils wound with 2g tapes and roebel cable: dependence on spacing between turns/strands," vol. 25, no. 3, p. 035002, publisher: IOP Publishing. [Online]. Available: https://doi.org/10.1088/0953-2048/25/3/035002

[12] E. Pardo, J. Šouc, and J. Kováč, "AC loss in ReBCO pancake coils and stacks of them: modelling and measurement," vol. 25, no. 3, p. 035003, publisher: IOP Publishing. [Online]. Available: https://doi.org/10.1088/0953-2048/25/3/035003

[13] Z. Jiang, N. J. Long, M. Staines, R. A. Badcock, C. W. Bumby, R. G. Buckley, and N. Amemiya, "AC loss measurements in HTS coil assemblies with hybrid coil structures," vol. 29, no. 9, p. 095011, publisher: IOP Publishing. [Online]. Available: https://doi.org/10.1088/0953-2048/29/9/095011

[14] A. Colle, T. Lubin, S. Ayat, O. Gosselin, and J. Leveque, "Test of a flux modulation superconducting machine for aircraft," vol. 1590, no. 1, p. 012052, publisher: IOP Publishing. [Online]. Available: https://doi.org/10.1088/1742-6596/1590/1/012052

[15] R. Dorget, A. Cipriani, J. Lévêque, W. Dirahoui, S. Ayat, T. Lubin, P. Gning, J. Labbé, J. Tanchon, and J. Lacapère, "Design and assembly of a 250 kW partially superconducting flux modulation machine," vol. 35, no. 5, pp. 1–6. [Online]. Available: https://ieeexplore.ieee.org/document/10878269/

[16] I. Cotton, R. Gardner, D. Schweickart, D. Grosean, and C. Severns, "Design considerations for higher electrical power system voltages in aerospace vehicles," in *2016 IEEE International Power Modulator and High Voltage Conference (IPMHVC)*. IEEE, pp. 57–61. [Online]. Available: http://ieeexplore.ieee.org/document/8012771/

[17] Y. Wang, X. Guan, and J. Dai, "Review of AC loss measuring methods for HTS tape and unit," vol. 24, no. 5, pp. 1–6, conference Name: IEEE Transactions on Applied Superconductivity. [Online]. Available: https://ieeexplore.ieee.org/abstract/document/6857989

[18] F. Grilli, E. Pardo, A. Stenvall, D. N. Nguyen, W. Yuan, and F. Gömöry, "Computation of losses in HTS under the action of varying magnetic fields and currents," vol. 24, no. 1, pp. 78–110, number: 1 Conference Name: IEEE Transactions on Applied Superconductivity. [Online]. Available: https://ieeexplore.ieee.org/abstract/document/6648727

[19] M. Furuse, J. Kondoh, H. Tanaka, and M. Umeda, "AC loss measurement of HTS coils with ferromagnetic disks," vol. 13, no. 2, pp. 2356–2359. [Online]. Available: https://ieeexplore.ieee.org/abstract/document/1212094